# 伯胺 $N_{1923}$ 萃淋树脂吸萃汞(Ⅱ)机理的研究*

程德平** 夏式均

(杭州大学化学系,杭州 310028)

**摘要** 研究伯胺 $N_{1923}$ 萃淋树脂在萃取剂 $N_{1923}$ 成盐和不成盐时不同条件下吸附汞的反应机理,通过等摩尔系列法、斜率法、饱和容量法等确定吸萃物在成盐和非成盐时的组成分别为:$(RNH_3^+)_2HgCl_4^{2-}$ 和 $(RNH)_2HgCl_2$。并通过红外光谱和核磁共振光谱分析吸萃过程中的不同机理:成盐时为离子交换机理,非成盐时为配位机理。

**关键词** 汞,机理,萃淋树脂,伯胺 $N_{1923}$。

伯胺 $N_{1923}$ 是萃取金属离子十分有效的萃取剂,Singh 等[1,2]曾报道叔碳伯胺 Primene JMT 萃取汞(Ⅱ)的研究,认为萃取机理是阴离子交换,但未能作详细深入的探讨。本文将萃取剂伯胺 $N_{1923}$ 制成萃淋树脂,将萃取剂的选择性和萃淋树脂的高效性有机地结合起来,详细研究了 $N_{1923}$ 萃淋树脂在成盐和不成盐情形下吸附汞的不同机理。因汞是引起环境污染的重要元素,研究萃淋树脂对其的吸萃行为和吸萃机理将可能在环境保护与治理方面探索出一条新途径。

## 1 实验部分

### 1.1 主要试剂与仪器

伯胺 $N_{1923}$ 由上海有机所实验厂提供($R_1R_2CHNH_2$,$R = C_{19-23}$,平均分子量为 280.69),$HgCl_2$ 溶液由分析纯试剂配成 1.0 mg/ml 汞标准溶液。

PE-683 型红外光谱仪,EM-90 型核磁共振仪,日本岛津 AA6501 型原子吸收分光光度计,THZ-82 型恒温振荡器。

### 1.2 $N_{1923}$ 萃淋树脂的制备

在干燥的 250 ml 烧杯中,各加入 25 g 苯乙烯、二乙烯苯(35.75%),适量偶氮二异丁腈,搅拌使引发剂完全溶解,再加 25 g $N_{1923}$ 萃取剂和适量的致孔剂,在上述油相搅拌均匀后,转入 500 ml 盛有 250 ml 去离子水、0.5 g 明胶、0.1 g 十二烷基苯磺酸钠的三颈瓶中,80℃反应 6 h,90℃反应 4 h,反应结束后,待温度降至 40℃,过滤、洗涤、干燥,筛取直径为 0.18—0.25 mm 大小的树脂备用。

树脂含氮量经元素分析,换酸成萃取剂含量为 1.35 mmol/g。

### 1.3 实验方法

预备实验表明,振荡 90 min $N_{1923}$ 萃淋树脂吸萃汞可达平衡。实验中准确称取树脂 100 mg 若干份,置于具塞锥形瓶中,加一定量汞标准液,以缓冲液或盐酸及 $NH_4Cl$ 调节氢离子或氯离子浓度,用去离子水稀释至 30 ml,在振荡器上振荡 90 min,取清液用原子吸收法测定残留汞量,差减法计算汞的分配比 $D$ 及吸萃百分率 $E$:

$D = (c_0 - c)V/Wc$; $E = (c_0 - c)/c \times 100\%$

式中,$V$ 是溶液体积(ml),$c_0$ 和 $c$ 分别为水相中汞的起始和平衡浓度,$W$ 为所取树脂的重量(g)。

文中实验条件除注明外,体系温度为 25±1℃,$[H^+]$、$[Cl^-]$ 分别为 0.1 mol/L,$N_{1923}$ 树脂负载量为 1.35 mmol/g。

## 2 结果与讨论

### 2.1 离子缔合机理

* 浙江省自然科学基金资助课题

** 通信联系人

收稿日期:1995-08-20

(1) $[Cl^-]$恒定时，$[H^+]$对汞吸附性能的影响　从图 1 可见，液相酸度≤0.1 mol/L 时，对汞吸附性能基本无影响。胺与盐酸作用易成盐，$K_H$ 较大[3]当 $N_{1923}$树脂用盐酸预平衡后，胺基本上转化为盐，在低酸度$[H^+]$≤0.1 mol/L 时，对汞(Ⅱ)的吸附反应为：

$$n\overline{RNH_2 \cdot HCl} + HgCl_4^{2-} \rightleftharpoons \overline{HgCl_4(RNH_3^+)_n} + nCl^- \quad (1)$$

$N_{1923}$萃淋树脂吸附汞的总量为 $\sum_{n=1}^{N}\overline{[HgCl_4(RNH_3^+)_n]}$，分配比

$$D = \sum_{n=1}^{N}\overline{[HgCl_4(RNH_3^+)_n]}/[HgCl_4^{2-}] \quad (2)$$

以 $K_n$ 式代入(2)式得：

$$D = [Cl^-]^{-n}\sum_{n=1}^{N}K_n\overline{[RNH_2HCl]^n}$$

取对数：

$$\lg D = \lg\sum_{n=1}^{N}(K_n\overline{[RNH_2 \cdot HCl]^n}) - n\lg[Cl^-] \quad (3)$$

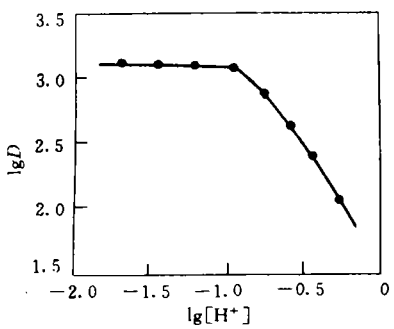


图 1　酸度对吸附性能的影响

(2) 斜率法　由(3)式作 $\lg D$-$\lg[RNH_2 \cdot HCl]$及 $\lg D$-$\lg[Cl^-]$图可确定 $n$ 值。从图 2 与图 3 所得直线斜率分别接近 2 或 −2，表明 $RNH_2 \cdot HCl$以双分子参加反应，或 2 个 $Cl^-$离子参与反应，即 $n=2$。

(3) 等摩尔系列法　称取不同量的 $N_{1923}$萃淋树脂几份，加入不同量的汞标准溶液使 $Hg^{2+}$与 $N_{1923}$的总摩尔数为 100 μmol，按吸附平衡法所得结果以吸附量 $Q$ 对应于$[Hg]/([Hg]+[\overline{N_{1923}}])$，可求得最大吸附量时，$[Hg]/([Hg]+[\overline{N_{1923}}])$为 0.34，说明吸萃物分子中含 2 个萃取剂 $N_{1923}$分子和 1 个汞离子，即 $n=2$。

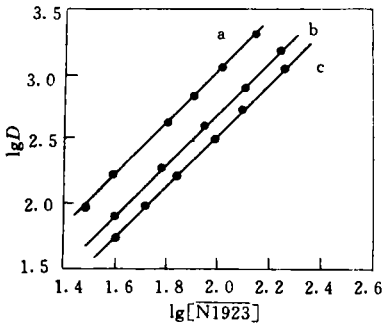


图 2　不同 $N_{1923}$负载量对分配比 $D$ 的影响

$[Cl^-]$：a. 0.04 mol/L　b. 0.10 mol/L　c. 0.30 mol/L

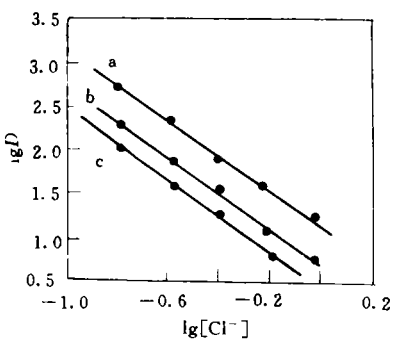


图 3　$[Cl^-]$对吸附性能的影响

$N_{1923}$负载量：a. 1.35 mmol/g

b. 1.09 mmol/g　c. 0.87 mmol/g

(4) 平衡移动法　准确称取 100 mg $N_{1923}$萃淋树脂若干份，加不同量(依次递增)Hg(Ⅱ)液，求得 $N_{1923}$树脂的饱和吸附容量为 0.61 mmol/g，与 $N_{1923}$的摩尔比为 1∶2，与斜率法、等摩尔系列法所得相符合。因此，吸附物分子组成确为$\overline{HgCl_4(RNH_3)_2}$，其反应类似于液液萃取中阴离子交换机理[4,5]：

$$HgCl_4^{2-} + 2\overline{RNH_2 \cdot HCl} \overset{K_2}{\rightleftharpoons} \overline{HgCl_4(RNH_3)_2} + 2Cl^- \quad (4)$$

$K_2$ 代表此反应的平衡常数。

## 2.2　未用盐酸酸化的 $N_{1923}$萃淋树脂机理

### 2.2.1　酸度对吸附性能的影响

以缓冲液或盐酸调节液相的初始酸度，未

酸化 $N_{1923}$萃淋树脂对汞的吸附性能，在微酸性 pH 为 2.0、3.0、4.0、5.0 介质中吸附性能基本未变，分配比 $D$ 值较大；酸度稍大时，在 $D$ 值 -lg[$H^+$]所作图中，当盐酸浓度增大至 pH 为1.0 时，$N_{1923}$萃淋树脂对汞的吸附分配比 $D$ 值急骤减小，因此，选择 pH 为 4 左右的酸度进行实验。

**2.2.2** 未成盐 $N_{1923}$萃淋树脂吸萃机理的探讨

假如 $N_{1923}$萃淋树脂对汞的吸附反应为：

$$HgCl_4^{2-} + i\overline{RNH_2} \overset{K'}{\rightleftharpoons} \overline{HgCl_{4-i}(RNH_2)^i} + iCl^- \quad (5)$$

分配比 $D=K'[RNH_2]^i/[Cl^-]^i$

取对数 $\lg D = \lg K' + i\lg[RNH_2] - i\lg[Cl^-]$ (6)

(1) 斜率法 在 pH＝4 的酸度条件下，研究不同负载量 $N_{1923}$以及氯离子浓度对汞吸附性能的影响。控制[$Cl^-$]为 0.05 和 0.30 mol/L 时，不同未成盐 $N_{1923}$树脂负载量对 $D$ 的影响，以 lg$D$-lg[$RNH_2$]作图所得的二直线斜率都接近于 2，说明 $i$ 值为 2。氯离子浓度对未成盐 $N_{1923}$萃淋树脂吸附性能的影响，以 lg$D$-lg[$Cl^-$]作图所得的直线斜率接近－2，也得 $i$=2 的结论。

(2) 等摩尔系列法 以确定 $N_{1923}$未成盐时对吸附物分子组成的影响，作等摩尔系列曲线，求得最大吸附量时[Hg]/([Hg]+[$\overline{N_{1923}}$])为 0.36，说明吸附物分子组成为 2 个 $N_{1923}$分子和 1 个汞原子，由此也可确认 $i$ 为 2。

因此，$N_{1923}$萃淋树脂未成盐情况下吸附汞的反应是由于伯胺空间位阻小而形成内配位的络合机理[6]：

$$HgCl_4^{2-} + 2\overline{RNH_2} \overset{K'}{\rightleftharpoons} \overline{HgCl_2[RNH_2]_2} + 2Cl^- \quad (7)$$

**2.3** 盐酸浓度对汞吸附机理的影响

从图 4 可以看出，盐酸浓度影响 $N_{1923}$萃淋树脂对 Hg(Ⅱ)的吸附机理。在 HCl 浓度高时，体系中存在着下述平衡：

$$HgCl_4^{2-} + H^+ \overset{K_H}{\rightleftharpoons} HHgCl_4^- \quad (8)$$

即 $N_{1923}$萃淋树脂吸附 $HgCl^{2-}$的同时，也可能吸附 $HHgCl_4^-$。

$$HHgCl_4^- + \overline{RNH_2 \cdot HCl} \overset{K_1}{\rightleftharpoons} \overline{RNH_3HHgCl_4} + Cl^- \quad (9)$$

此时：

$$D = \frac{\overline{[RNH_3 \cdot HHgCl_4]} + \overline{[(RNH_3)_2HgCl_4)]}}{[HHgCl_4^-] + [HgCl_4^{2-}]} \quad (10)$$

从(8)式可得：

$$K_H = [HHgCl_4^-]/\{[HgCl_4^{2-}][H^+]\} \quad (11)$$

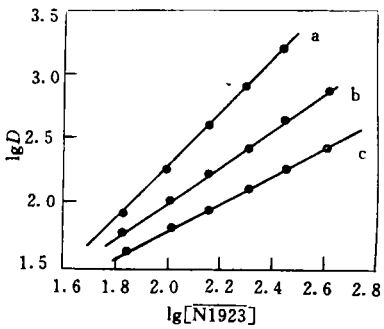


图 4 盐酸浓度对吸附机理的影响

[HCl]: a. 0.1 mol/L; b. 0.3 mol/L; c. 0.5 mol/L

若令：

$$m = [HHgCl_4^-]/[HgCl_4^{2-}] = K_H[H^+] \quad (12)$$

$$n = \overline{[RNH_3 \cdot HHgCl_4]}/\overline{[(RNH_3)_2HgCl_4]} \quad (13)$$

从式(9)与式(4)可得

$$\frac{K_1}{K_2} = \frac{\overline{[RNH_3 \cdot HHgCl_4]}[HgCl_4^{2-}]\overline{[RNH_2 \cdot HCl]}}{\overline{[(RNH_3)_2HgCl_4]}[HHgCl_4^-][Cl^-]} \quad (14)$$

将(12)、(14)式代入(13)式可得：

$$n = K_1K_H[H^+][Cl^-]/\{K_2[RNH_2 \cdot HCl]\} \quad (15)$$

以(11)、(12)代入(10)整理得：

$$D = [(1+n)/(1+m)] \cdot \overline{[(RNH_3)_2HgCl_4]}/[HgCl_4^{2-}] \quad (16)$$

由[4]式得：

$$K_2 = \frac{\overline{[(RNH_3)_2HgCl_4]}[Cl^-]^2}{[HgCl_4^{2-}]\overline{[RNH_2 \cdot HCl]}^2} \quad (17)$$

将(17)式代入(16)式，即：

$$D = [(1+n)/(1+m)] \cdot K_2[\overline{RNH_2 \cdot HCl}]^2 /[Cl^-] \quad (18)$$

将(18)式偏微分，得：

$$\{\partial \lg D/[\partial \lg(\overline{RNH_2 \cdot HCl})]\}_{[H^+][Cl^-]} = 1 + 1/(1+n) \quad (19)$$

由(19)式可见，$\lg D$-$\lg[\overline{RNH_2 \cdot HCl}]$直线的斜率取决 $n$ 值，在低酸度时，$n$ 值可忽略，斜率接近于 2，在盐酸浓度较高时，$n$ 值增大，斜率在 2—1 之间，趋向于 1，这与实验所得的图 4 相一致。

**2.4** 红外光谱与核磁共振光谱分析

为了进一步确证 2 种不同键合类型吸萃物的吸萃机理，进行了红外和核磁共振谱的分析研究。IR 图谱(见图 5)表明，$\overline{RNH_2}$中的 $\nu^{as}_{(NH)}$，$\nu^{s}_{(NH)}$，$\delta^{内}_{(NH)}$峰分别在 3370、3300 和 1620 $cm^{-1}$处出现，生成$\overline{HgCl_2(RNH_2)_2}$后，仍出现—$NH_2$ 基中的 N-H 振动，但吸收峰的位置分别移至 3209、3109 和 1537 $cm^{-1}$。这说明 $RNH_2$ 是以配位键的形式和 Hg(Ⅱ)结合，从而导致 N-H 键强度减弱，而在吸萃物$\overline{HgCl_4(RNH_3)_2}$中，N-H 振动表现出$-NH_3^+$ 的特征，在 1600、1495 $cm^{-1}$ 处出现了$-NH_3^+$ 的 2 个弯曲振动峰，说明在吸萃物中，胺是以$-NH_3^+$ 形式存在的。

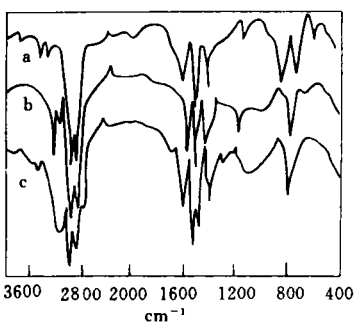


图 5　红外光谱图

a. $\overline{RNH_2}$　b. $\overline{HgCl_2(RNH_2)_2}$　c. $\overline{HgCl_4(RNH_3)_2}$

NMR 谱如图 6，$\overline{RNH_2}$的 NMR 谱表明—$NH_2$上的$^1H$ 化学位移为 1.15 ppm，与 N 相连的仲碳上的$^1H$ 化学位移为 2.47 ppm。形成$\overline{HgCl_2 \cdot (RNH_2)_2}$后，它们分别移至 4.58 和 3.45 ppm 处，进一步证实了$\overline{RNH_2}$是以配位键和 Hg(Ⅱ)结合的，配位后，氮离子周围的电子云密度减小，导致与其相连的氢原子屏蔽作用变小，从而使$^1H$ 的化学位移向低场方向，同样，仲碳上的$^1H$ 峰亦产生移动。$\overline{HgCl_4 \cdot (RNH_3)_2}$的核磁共振谱表明与氮相连的$^1H$ 峰出现在 7.00 ppm 处，确认了在萃合物中胺是以 $RNH_3^+$ 的形式存在。从 IR 和 NMR 谱的分析进一步说明在 $N_{1923}$萃淋树脂吸萃 Hg(Ⅱ)的过程中确实存在上述 2 种机理。

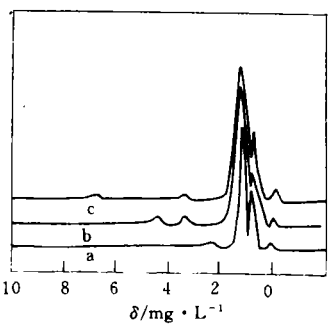


图 6　核磁共振光谱

a. $\overline{RNH_2}$　b. $\overline{HgCl_2(RNH_2)_2}$　c. $\overline{HgCl_4(RNH_3)_2}$

## 参 考 文 献


1　Singh O V, Tandon S N. Sep. Sci., 1975, **10**(4): 359

2　Singh O V, Tandon S N. J. Inorg. Nucl. Chem., 1974, **36**: 439

3　庄文德. 分析化学, 1975, **3**(2): 156

4　乐少明, 李德谦, 倪嘉缵. 无机化学, 1987, **3**(2): 80

5　乐少明, 李德谦. 倪嘉缵. 应用化学, 1987, **4**(1): 26

6　沈静兰, 盖会发等. 贵金属, 1986, **7**(1): 6

HUANJING KEXUE

Abstracts Environmental Science Vol. 17 No. 2, 1996

**A Research on the Ecological Effect of the Soil Animals Community by the Heavy Metal Pollution.** Deng Jifu et al. (Zhuzhou Institute of Environ. Sci., Zhuzhou 412000): *Chin. J. Environ. Sci.*, **17**(2), 1996, pp. 1—5

The research results show that there are 31 soil animal species in the polluted area, in which *Acarina* and *Collembola* are dominant population. The species and quantities of the soil animals are decreased with the aggravation of pollution, which can be found mainly from the growth and decline of the dominant population and decrease and disappearance of the polluted sensitive species. The big animals, such as earthworm and spider, have a strong ability to acculate heavy metal elements. The content of Cd、Pb、As in these animal's body relates proportionally to the metals in soil, but the centipede's ability in accumulating the heavy metal elements is abviously weaken.

**Key words**: heavy metal pollution, soil animal, ecological distribution, accumulation.

**Microbial Degradation of Regenerated Cellulose Film.** Zheng Lianshuang et al. (Dept. of Environ. Sci. Wuhan University, Wuhan 430072): *Chin. J. Environ. Sci.*, **17**(2), 1996, pp. 6—8

The biodegradability of regenerated cellulose film was tested by soil-burial test in field, culture-dish test and $CO_2$ evolution test respectively. The results of test are as follows: (1) The mass loss of the film increased with the extension of soil-burial test; (2) Test strains had different abilities to degrade the film, and the order of their abilities was strain T-311>strain A-305>strain P-307; the biodegradation rate of the film might exceed 70% during 42 days after the film had been buried or inoculated with strain T-311; (4) In the process of biodegradation, mass loss, visible growth of test strains on the film and $CO_2$ evolution are both relative and different indexes for assessing biodegradation degrees of the film.

**Key words**: regenerated cellulose film, biodegradability, $CO_2$ evolution.

**Adsorption Behavior of Ammonnium Ion in Saturated Silty Sand and Sandy Loam.** Zhu Wanpeng et al. (Dept. of Environ. Eng., Tsinghua University, Beijing 100084): *Chin. J. Environ. Sci.*, **17**(2), 1996, pp. 9—11

The adsorption characteristics of ammonium ion in saturated silty sand and sandy loam were studied by means of dynamic soil column experiments. The transportation of ammonium ion in soil were modelled with a combined equilibrium and kinetic adsorption model (Cameron's model). The coefficients ($K_1$, $K_2$ and $K_3$) under different soil and $NH_4^+$ concentration in water were obtained. The distribution curves of ammonium ion in soil were drawn. The results indicate that the longitudinal dispersion coefficients ($D$) in silty sand and sandy loam are 0.175 $cm^2$/min and 0.0093 $cm^2$/min respectively. The dynamic adsorption capacity of silty sand are 0.156 mg/g when concentration of $NH_4^+$ in water is 13.7 mg/L and 0.400 mg/g when concentration of $NH_4^+$ in water is 41.0 mg/L; the dynamic adsorption capacity of sandy loam is 1.33 mg/g when concentration of $NH_4^+$ in water is 51.0 mg/L. Above results can be used to determine the suitable thickness of protective soil in land treatment system of wastewater.

**Key words**: ammonium ion, saturated silty sand, saturated sandy loam, transportation, dynamic soil column experiment.

**Study on the Adsorption Mechanism of Mercury (Ⅰ) with Prime Amine $N_{1923}$ Levextrel Resin.** Cheng Deping and Xia Shijun (Dept. of Chem., Hangzhou University, Hangzhou 310028): *Chin. J. Environ. Sci.*, **17**(2), 1996, pp. 12—15

The adsorption mechanisms of mercury (Ⅰ) with prime amine ($N_{1923}$) levextrel resin were studied when it doesn't form salt or it is in salt forming condition. The adsorption compounds have been determined and the different mechanisms have been analysed from the results obtained by using constant mole method, slope method, saturated capacity method, IR and NMR spectra, and also discussed the different mechanism in low or high concentration of [HCl] on the theroy.

**Key words**: mercury, mechanism, levextrel resin, primary amine $N_{1923}$.

**A Study on Effects of Simulated Acid Rain and Sulphur Dioxide on Crops.** Liu Liangui et al. (Chinese Research Academy of Environmental Sciences, Beijing 100012): *Chin. J. Environ. Sci.*, **17**(2), 1996, pp. 16—19

The effects of acid rain and sulphur dioxide alone and in combination on tomato, carrot and cotton was studied by simulated acid rain irrigating and $SO_2$ exposure. It was found that the simulated acid rain and sulfur dioxide could inhibit the growth of crops in a degree and reduce the productivity. The synthetic effect of acid rain and sulfur dioxide was more notable than alone, but their mutual effect was not marked.

**Key words**: simulated acid rain, sulfur dioxide, crop, inhibition, synthetic effect.

**The Fluxes of Volatile Mercury over Soil Surface in Guizhou Province.** Feng Xinbin et al. (State key Laboratory of Environmental Geochemistry, Institute of Geochemistry, Chinese Academy of Sciences, Guiyang, 550002): *Chin. J. Environ. Sci.*, **17**(2), 1996, pp. 20—22

After summing up the work of former researchers, the authors set up a instrument which can be used to measure the fluxes of volatile mercury over soil in field. From Aug. to Oct. in 1993, the authors studied the fluxes of volatile mercury over soil at five sites of three different areas (high mercury contented area, mercury polluted area and reference area). Studies showed that soil release more volatile mercury in day than at night, and that the fluxes of volatile mercury over soil has relationship with both the total mercury content of soil and air temperature.

**Key words**: mercury, fluxes, flux chamber, Guizhou